Advanced Study Workshop on Earthquake Engineering

Numerical Modeling of Dispersed Particle Motion in Pipelines with Abrupt Contractions

AIPCP25-CF-ASWEE2025-00038 | Article

Comparison of the Results of Applying a Two-Fluid Turbulence Model with One and Two-Equation Turbulence Models to the Problem of a Subsonic Axisymmetric Submerged Jet

Sardor Khaydarov[1,a)] and Zafar Malikov[2,b)]

[1]*Andijan state technical institute, 170119, Andijan, Baburshox st. 56, Uzbekistan*
[2]*Institute of Mechanics and Seismic Stability of Structures named after M.T.Urazbaev, Uzbekistan Academy of Sciences, 100125, Tashkent, Dormon yuli, 40, Uzbekistan.*

[a)] Corresponding author: khaydarovsardor@gmail.com
[b)] malikov.z62@mail.ru

Abstract. This article explores an axisymmetric subsonic jet using modern turbulence models. Despite its simplicity, this problem is quite challenging for turbulence modeling. Therefore, many current RANS models are unable to even qualitatively describe such problems. A comparative analysis of the vt-92, Menter's k-ω (SST), and two-fluid turbulence models is performed for a submerged axisymmetric subsonic jet. An implicit scheme was used for the numerical implementation of the problem. The comparative analysis was performed for axial velocity, longitudinal velocities at different cross sections from the nozzle, transverse velocity, and turbulent stress. The obtained numerical results are compared with NASA experimental data. It is shown that the two-fluid turbulence model more accurately describes turbulent flow than other turbulence models.

INTRODUCTION

The problem under research holds significant relevance for both aviation and aerospace engineering, which has motivated extensive research on jet flows over the past century, beginning with the pioneering studies of Prandtl [1,2]. Nevertheless, despite the considerable progress made, the issue cannot be regarded as fully resolved, largely due to the persistent challenges associated with turbulence modeling. Advanced approaches such as Direct Numerical Simulation (DNS) [3,4] and Large Eddy Simulation (LES) [5,6] offer valuable insights into turbulent flows but remain computationally demanding. Their application to complex engineering problems in aerodynamics requires access to high-performance computing resources, and thus, widespread adoption is likely to depend on further advances in computational technologies, potentially becoming feasible only toward the end of the century. Consequently, for the foreseeable future, semi-empirical methods will continue to serve as the primary practical tools for addressing applied aerodynamic problems.

Although more than one hundred turbulence models have been proposed to date, a universally applicable model has yet to be established. This limitation arises from the fact that a model capable of adequately capturing one class of flows may yield inaccurate, or even qualitatively incorrect, results when applied to another. In many fluids dynamic problems involving liquids and gases, tangential discontinuity surfaces frequently occur, giving rise to jet flows in their vicinity. Depending on the relative flow directions, jets can be classified as either co-flowing or counter-flowing. Among these, the most extensively investigated configuration is the jet discharging into a quiescent ambient medium, commonly referred to as a submerged jet [7]. In the present study, a comparative assessment is conducted between the Secundov vt-92 [8], Menter's k−ω (SST) [9,10] and two-fluid turbulence models for an axisymmetric subsonic jet [11–23]. This configuration is particularly advantageous for analysis, as it closely approximates realistic subsonic jet

conditions encountered in aircraft engine turbines, while also being supported by comprehensive experimental datasets [24].

TURBULENCE MODELS

Two-fluid model

The governing equations for an incompressible turbulent jet, formulated within the framework of the two-fluid model and expressed in cylindrical coordinates, can be written as follows [12]:

$$\begin{cases} \frac{\partial U}{\partial t}+U\frac{\partial U}{\partial x}+V\frac{\partial U}{\partial r}+\frac{\partial p}{\rho\partial x}=\nu\left(\frac{\partial^2 U}{\partial r^2}+\frac{\partial U}{r\partial r}+\frac{\partial^2 U}{\partial x^2}\right)-\frac{\partial r\vartheta u}{r\partial r}-\frac{\partial uu}{\partial x}, \\ \frac{\partial V}{\partial t}+U\frac{\partial V}{\partial x}+V\frac{\partial V}{\partial r}+\frac{\partial p}{\rho\partial r}=\nu\left(\frac{\partial^2 V}{\partial r^2}+\frac{\partial V}{r\partial r}+\frac{\partial^2 V}{\partial x^2}\right)-\frac{\partial r\vartheta\vartheta}{r\partial r}-\frac{\partial u\vartheta}{\partial x}, \\ \frac{\partial u}{\partial t}+U\frac{\partial u}{\partial x}+V\frac{\partial u}{\partial r}=-\frac{\partial U}{\partial x}u-\frac{\partial U}{\partial r}\vartheta+C_S\left(\frac{\partial U}{\partial r}-\frac{\partial V}{\partial x}\right)\vartheta+\frac{\partial}{\partial x}\left(2\nu_{xx}\frac{\partial u}{\partial x}\right)+\frac{\partial}{r\partial r}\left(\nu_{xr}r\left(\frac{\partial u}{\partial r}+\frac{\partial\vartheta}{\partial x}\right)\right)-K_f u, \\ \frac{\partial\vartheta}{\partial t}+U\frac{\partial\vartheta}{\partial x}+V\frac{\partial\vartheta}{\partial r}=-\frac{\partial V}{\partial r}\vartheta-\frac{\partial V}{\partial x}u-C_S\left(\frac{\partial U}{\partial r}-\frac{\partial V}{\partial x}\right)u+\frac{\partial}{\partial x}\left(\nu_{xr}\left(\frac{\partial\vartheta}{\partial x}+\frac{\partial u}{\partial r}\right)\right)+\frac{\partial}{r\partial r}\left(2\nu_{rr}r\frac{\partial\vartheta}{\partial r}\right)-2\nu_{rr}r\frac{\vartheta}{r^2}-K_f\vartheta, \\ \frac{\partial U}{\partial x}+\frac{\partial rV}{r\partial r}=0. \end{cases} \quad (1)$$

Here

$$\nu_{xx}=\nu_{rr}=3\nu+2\frac{S}{\mathrm{def}(\vec{V})},\ \nu_{xr}=3\nu+2\left|\frac{u\vartheta}{\mathrm{def}(\vec{V})}\right|,\ \mathrm{def}(\vec{V})=\sqrt{\left(\frac{\partial U}{\partial r}+\frac{\partial V}{\partial x}\right)^2+2\left(\frac{\partial U}{\partial x}\right)^2+2\left(\frac{\partial V}{\partial r}\right)^2},$$

$$S=\frac{u^2J_x+\vartheta^2J_r}{J_x+J_r},\quad J_x=\left|\frac{\partial u}{\partial x}\right|,\quad J_r=\left|\frac{\partial\vartheta}{\partial r}\right|,\quad C_s=0.2,\quad K_f=C_1\lambda_{\max}+C_2\frac{|d\cdot\vartheta|}{d^2}.$$

In expression (1), U, V – are the averaged axial and radial components of the flow velocity vector, respectively, u, ϑ – are the relative axial and radial velocities, respectively, ν_{xx}, ν_{rr} and ν_{xr} – are the effective molar viscosities, K_f – is the friction coefficient, and d – is the closest distance to the wall.

k-ω (SST) model

The *k-ω* model (SST) is a two-equation eddy-viscosity model developed by Menter (1994) to improve the accuracy of turbulence predictions in flows with adverse pressure gradients, separation, and near-wall effects. It blends the strengths of the standard $k-\omega$ and $k-\varepsilon$ models using a blending function [9,10].

$$\begin{cases} \frac{\partial k}{\partial t}+U\frac{\partial k}{\partial z}+V\frac{\partial k}{\partial r}=\frac{\partial}{r\partial r}\left[(\mu+\sigma_k\mu_t)r\frac{\partial k}{\partial r}\right]+P-\beta^*\omega k, \\ \frac{\partial\omega}{\partial t}+U\frac{\partial\omega}{\partial z}+V\frac{\partial\omega}{\partial r}=\frac{\partial}{r\partial r}\left[(\mu+\sigma_\omega\mu_t)r\frac{\partial\omega}{\partial r}\right]+\frac{\gamma}{v_t}P-\beta\omega^2+2(1-F_1)\frac{\sigma_{\omega2}}{\omega}\frac{\partial\omega}{\partial r}\frac{\partial k}{\partial r}, \end{cases} \quad (2)$$

In this expression

$$P=\tau\left(\frac{\partial U}{\partial r}\right),\ \tau=\nu_t\left(2S\right),\ S=\frac{1}{2}\left(\frac{\partial U}{\partial r}+\frac{\partial V}{\partial z}\right),\ \nu_t=\frac{a_1 k}{\left(a_1\omega,\ \ \Omega F_2\right)},\ \varphi=F_1\varphi_1+(1-F_1)\varphi_2,$$

$$F_1=\tanh\left(\arg_1^4\right),\ \ \arg_1=\min\left[\max\left(\frac{\sqrt{k}}{\beta^*\omega d},\frac{500}{d^2\omega}\right),\frac{4\sigma_{\omega 2}k}{CD_{kw}d^2}\right],$$

$$CD_{kw}=\max\left(2\sigma_{\omega 2}\frac{1}{\omega}\frac{\partial k}{\partial r}\frac{\partial\omega}{\partial r},10^{-20}\right),\ F_2=\tanh\left(\arg_2^2\right),\ \arg_2=\max\left(2\frac{\sqrt{k}}{\beta^*\omega d},\frac{500}{d^2\omega}\right),$$

$$\Omega=\sqrt{2W*W},\ \ W=\frac{1}{2}\left(\frac{\partial U}{\partial r}+\frac{\partial V}{\partial z}\right),\ \omega_{wall}=10\frac{6\nu}{\beta_1\left(\Delta d\right)^2},$$

$$k_{wall}=0,\ \gamma_1=\frac{\beta_1}{\beta^*}-\frac{\sigma_{\omega 1}K^2}{\sqrt{\beta^*}},\quad \gamma_2=\frac{\beta_2}{\beta^*}-\frac{\sigma_{\omega 2}K^2}{\sqrt{\beta^*}}.$$

In addition to the auxiliary functions, the Minter turbulence model has the following empirical constants

$$\sigma_{k1}=0.85,\sigma_{\omega 1}=0.5,\ \beta_1=0.075,\ \sigma_{k2}=1,\sigma_{\omega 2}=0.856,\beta_2=0.0828,\beta^*=0.09,K=0.41,a_1=0.31.$$

ν_t-92 model

ν_t-92 is a one-equation eddy-viscosity turbulence model.

$$\begin{cases}\dfrac{\partial u}{\partial x}+\dfrac{\partial rv}{r\partial r}=0,\\ \dfrac{\partial u}{\partial t}+u\dfrac{\partial u}{\partial x}+v\dfrac{\partial u}{\partial r}=\dfrac{\partial}{r\partial r}\left(r(\nu+\nu_t)\dfrac{\partial u}{\partial r}\right),\\ \dfrac{\partial\rho\nu_t}{\partial t}+\dfrac{\partial(\rho u_j\nu_t)}{\partial x_j}=\rho(P_\nu-D_\nu)+\dfrac{\partial}{\partial x_j}\left[\rho(\nu+C_0\nu_t)\dfrac{\partial\nu_t}{\partial x_j}\right]+\dfrac{\partial}{\partial x_j}\left[\rho(-\nu+(C_1-C_0)\nu_t\right]\dfrac{\partial\nu_t}{\partial x_j}.\end{cases}\tag{3}$$

This model is based on the assumption that the vortex structure of the flow is transferred by convection and diffusion. Therefore, this model uses the substance transport equation to find the turbulent kinematic viscosity. Numerous studies of this model have shown that it is a low-Reynolds number model, meaning that it is capable of describing the entire flow region, including the near-wall layers. The first version of the Secundov νt-92 model was proposed in 1992 and has been improved over the years [8]. The model in cylindrical coordinates is written as (3). Here

$$P_\nu=\rho C_2A_2(\nu_t\Gamma_1+A_1\nu_t^{4/3}\Gamma_2^{2/3})+\rho C_2F_2A_2N_1\sqrt{(\nu+\nu_t)\Gamma_1}+\rho C_3\nu_t\left(\frac{\partial^2\nu_t}{\partial x_j\partial x_j}+N_2\right),$$

$$D_\nu=\rho C_5\nu_t^2\Gamma_1^2/a^2+\rho C_4\nu_t\left(\frac{\partial\langle u_j\rangle}{\partial x_j}+\left|\frac{\partial\langle u_j\rangle}{\partial x_j}\right|\right),$$

ν, ν_t – are the molecular and turbulent viscosity respectively; ɑ – is the speed of sound; angle brackets represent the values averaged over time. Turbulent eddy viscosity is determined by the formula $\mu_t=\rho\nu_t$.

Other quantities occurring in the above equations are defined as:

$$F_1 = \frac{N_1 d_w + 0.4 C_8 \nu}{\nu_t + C_8 \nu + \nu_{t,w}}, \qquad F_2 = \frac{\chi^2 + 1.3\chi + 0.2}{\chi^2 - 1.3\chi + 1.0}, \qquad \chi = \frac{\nu_t}{7\nu},$$

$$\Gamma_1 = \sqrt{\frac{\partial u_i}{\partial x_j}\left(\frac{\partial u_i}{\partial x_j} + \frac{\partial u_j}{\partial x_i}\right)}, \quad \Gamma_2 = \sqrt{\sum_i \left(\frac{\partial^2 u_i}{\partial x_j \partial x_j}\right)^2} = \sqrt{\left(\frac{\partial^2 u_i}{\partial x_n \partial x_n}\right) + \left(\frac{\partial^2 u_i}{\partial x_m \partial x_m}\right)},$$

$$N_1 = \sqrt{\frac{\partial \nu_t}{\partial x_j}\frac{\partial \nu_t}{\partial x_j}}, \qquad N_1 = \sqrt{\frac{\partial N_1}{\partial x_j}\frac{\partial N_1}{\partial x_j}}$$

$A_1 = -0.5,\ A_2 = 4.0,\ C_0 = 0.8,\ C_1 = 1.6,\ C_2 = 0.1,\ C_3 = 4.0,\ C_4 = 0.35,$

$C_5 = 3.5,\ C_6 = 2.9,\ C_7 = 31.5,\ C_8 = 0.1.$

NUMERICAL METHOD

In most cases, two-dimensional methods were used to numerically study the system of equations (1), (2) and (3). Furthermore, to achieve the required accuracy near the wall, the computational grid was refined in the transverse direction. This resulted in increased memory requirements for the required program and a slower calculation speed. Therefore, developing a numerical algorithm that does not require extensive computational resources is a pressing task. For the numerical study of this problem, a system of equations, the Reynolds-averaged Navier-Stokes equations in a cylindrical coordinate system, is used [25]. For numerical implementation, the system of equations (1)-(3) was reduced to a dimensionless form by correlating all velocities to the average jet velocity at the nozzle outlet U_{jet}, and linear dimensions to the nozzle radius R. The study was conducted for a jet with a Reynolds number 5600.

For this problem, we introduce a generalized stream function, for which the following relations hold:

$$u = \frac{\psi \partial \psi}{r \partial r}, \quad v = -\frac{\psi \partial \psi}{r \partial x}. \tag{4}$$

Here x and r are the dimensionless longitudinal and radial coordinates. The initial and boundary conditions for the system of equations (1) - (3) are set in the standard manner [7].

We write the all system of equations in von Mises variables (x, r) by (ξ, η), where $\xi = x / L$. In the new variables, the derivatives are determined by known formulas as:

$$\frac{\partial}{\partial x} = \frac{\partial \xi}{\partial x}\frac{\partial}{\partial \xi} + \frac{\partial \psi}{\partial x}\frac{\partial}{\partial \psi}, \qquad \frac{\partial}{\partial r} = \frac{\partial \xi}{\partial r}\frac{\partial}{\partial \xi} + \frac{\partial \psi}{\partial r}\frac{\partial}{\partial \psi}. \tag{5}$$

RESULTS AND DISCUSSION

Figure 1 shows a comparison of the results of turbulent models with experimental data from the dimensionless axial velocity as a function of the distance to the nozzle. From this figure it is evident that the closest results to the experimental data are given by the two-fluid model.

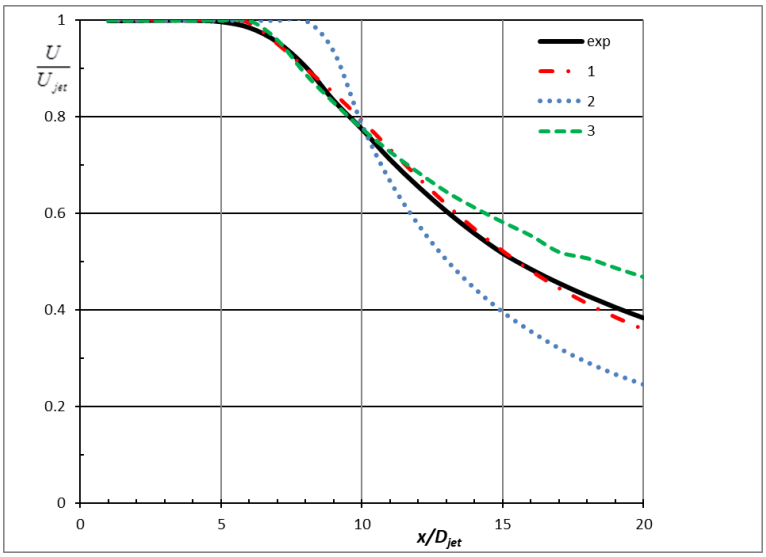

FIGURE 1. Comparison of turbulent model results with experimental data for dimensionless axial velocity as a function of distance to the nozzle. 1-two-fluid model, 2- *k-ω* (SST) model, 3- vt-92 model.

Figure 2 illustrates the results of turbulent models and experimental data for dimensionless longitudinal velocity profiles at different distances from the nozzle.

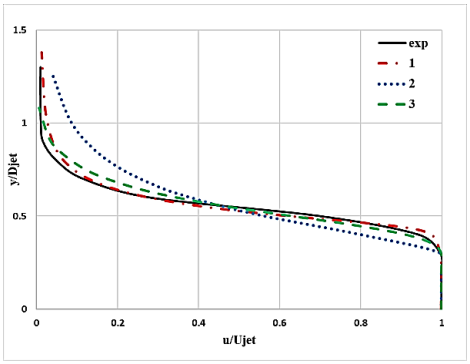

$x/D_{jet}=2$

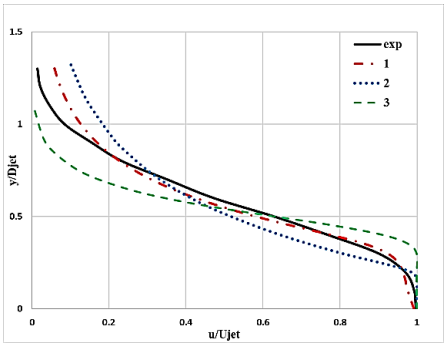

$x/D_{jet}=5$

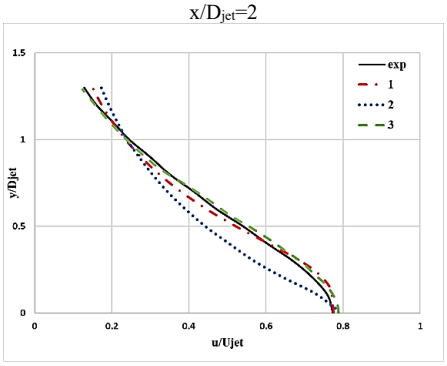

$x/D_{jet}=10$

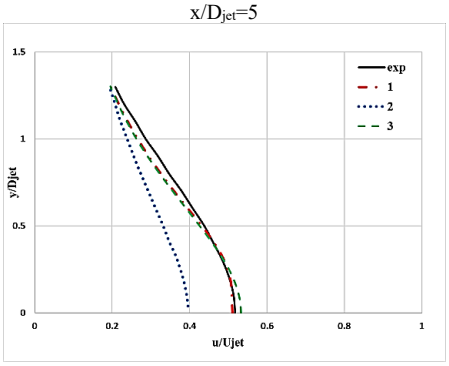

$x/D_{jet}=15$

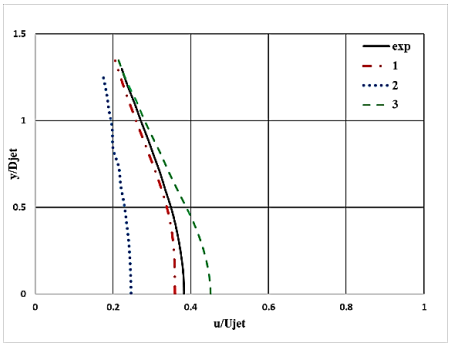

FIGURE 2. Comparison of the results of longitudinal velocity profiles for different sections from the nozzle. 1- two-fluid model, 2- k-ω (SST) model, 3- νt-92 model

$x/D_{jet}=20$

Figure 3 shows the results of turbulent models and experimental data for dimensionless transverse velocity profiles at different distances from the nozzle.

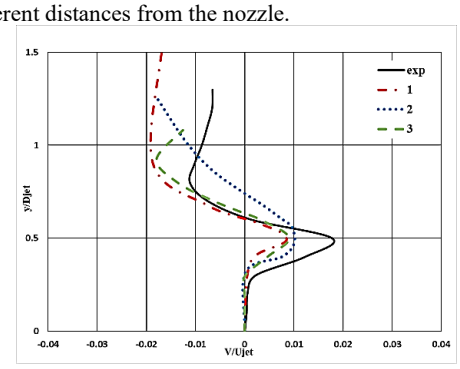

$x/D_{jet}=2$

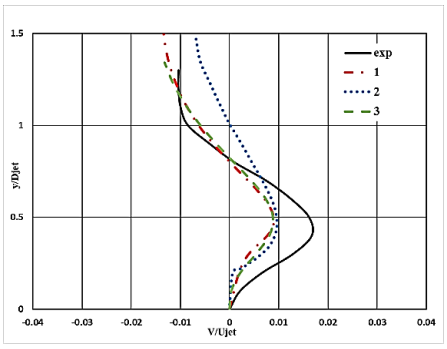

$x/D_{jet}=5$

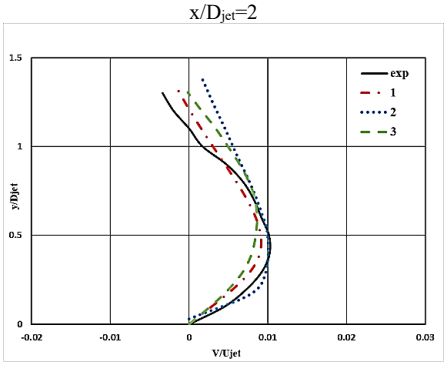

$x/D_{jet}=10$

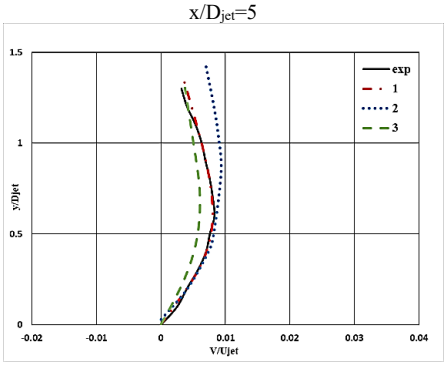

$x/D_{jet}=15$

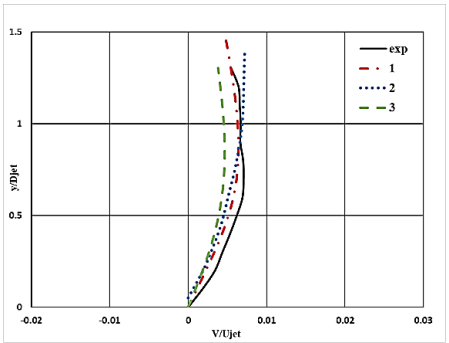

FIGURE 3. Comparison of the results of transverse velocity profiles for different sections from the nozzle. 1- two-fluid model, 2- k-ω (SST) model, 3- vt-92 model.

$x/D_{jet}=20$

Figure 4 illustrates the results of turbulent models and experimental data for turbulent stress profiles at different distances from the nozzle. From all the figures it is clear that the results obtained by the two-fluid model are very close to the experimental data, although the other two models also give satisfactory results. In particular, the results of vt-92 model in some cases are same with the two-fluid model.

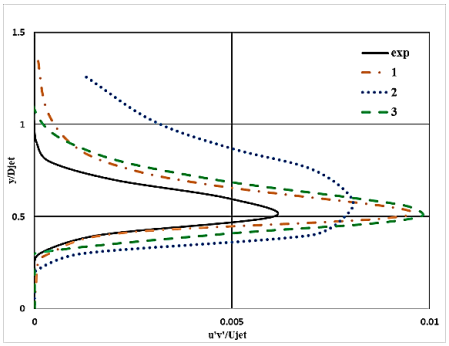

$x/D_{jet}=2$

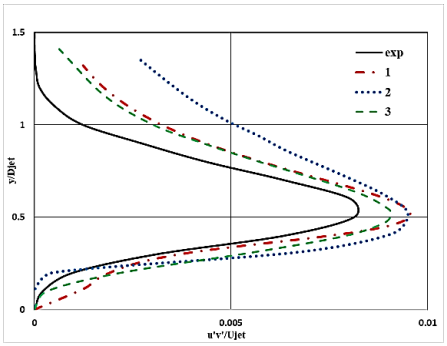

$x/D_{jet}=5$

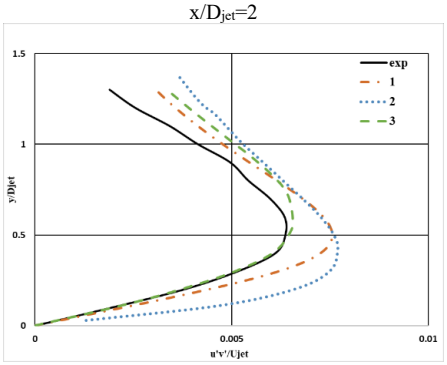

$x/D_{jet}=10$

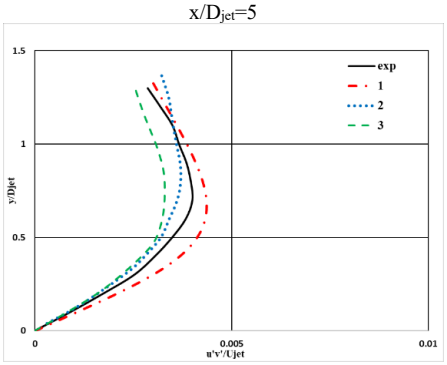

$x/D_{jet}=15$

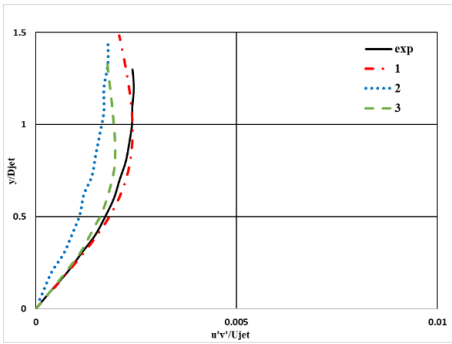

x/D_{jet}=20

FIGURE 4. Comparison of the results of turbulent stress profiles for different sections from the nozzle. 1-two-fluid model, 2- k-ω (SST) model, 3- vt-92 model.

CONCLUSION

A comparative test of the model vt-92, *k-ω* (SST) turbulence model, and the two-fluid model was conducted using experimental results from the NASA database. It was shown that the two-fluid model adequately describes the turbulent jet in all flow regions. Furthermore, the two-fluid model and the vt-92 model do not exhibit the round jet anomaly, compared to the Minter k-ω turbulence model. Unsatisfactory results were observed for the k-ω model in the terminal regions. Therefore, the two-fluid model can be recommended for calculating jet flows.

ACKNOWLEDGMENTS

This study was made possible by budget funding from the Uzbekistan Academy of Sciences. We express our sincere gratitude to the Academy for its ongoing support and commitment to advancing scientific research.

REFERENCES

1. G. N. Abramovich, The Theory of Turbulent Jets (The MIT Press) (2003).
2. S. B. Pope, Turbulent Flows (Cambridge University Press, Cambridge, 2000).
3. V. Maupu, D. Laurence, E. Boudjemadi, and P. Le Quere, (2025).
4. T. A. M. Versteegh and F. T. M. Nieuwstadt, Int. J. Heat Fluid Flow **19, 135** (1998).
5. C. Bogey and C. Bailly, Int. J. Heat Fluid Flow **27**, 603 (2006).
6. N. S. Ghaisas, D. A. Shetty, and S. H. Frankel, J. Turbul. **16**, 772 (2015).
7. P. Bradshaw, D. H. Ferriss, and N. P. Atwell, J. Fluid Mech. **28**, 593 (1967).
8. A. Gulyaev, V. Koziov, A. Secundov, M. Shur, M. Strelets and L. Zaikov, AIAA J **95**-0863 (1995)
9. F. R. Menter, Fluid Dyn. (1993).
10. F. R. Menter, AIAA J. **32**, 1598 (1994).
11. Z. Malikov, Appl. Math. Model. **82**, 409 (2020).
12. Z. M. Malikov, D. Navruzov, K. Adilov, and S. R. Juraev, in Proc. SPIE (2022), p. 44.
13. Z. Malikov, F. Nazarov, and S. Khaydarov, J. Appl. Comput. Mech. **11**, 871 (2025).
14. S. Khaydarov, "Application of a modern two-fluid turbulence model for methane-air simple jet combustion" in the *international conference: "Ensuring seismic safety and seismic stability of buildings and structures, applied problems of mechanics*" AIP Conf. Proc., edited by Abirov (AIP Publishing LLC, 2025), 3265.
15. Nazarov F. K. et al. "Calculation of axisymmetric transonic jet with various turbulence models using Comsol multiphysics package" in *XV International Online Conference "Improving Farming Productivity and Agroecology – Ecosystem Restoration" (IPFA 2023)*, edited by Bozarov (AIP Publishing LLC, 2025), 040040.
16. Malikov Z., Nazarov F. "Numerical study of flow on a flat plate with zero pressure gradient based on a two-fluid model" in the *international conference: "Ensuring seismic safety and seismic stability of buildings and structures, applied problems of mechanics*" AIP Conf. Proc., edited by Abirov (AIP Publishing LLC, 2025), 060003.
17. Nazarov F. K. et al. Comp. Res. Modeling, **T. 16, №. 5**, 1125-1142 (2024).

18. F. Nazarov et al., “Numerical calculation of turbulent flow in a two-dimensional flat diffuser based on the Comsol Multiphysics software,” in *Proceedings of the 7th International Conference on Future Networks and Distributed Systems,* edited by Mohammad Hammoudeh (Association for Computing Machinery, New York NY United States, 2023), pp. 372–376.
19. Nazarov et al., “Numerical study of laminar flow using various difference schemes,” in *Proceedings of the 7th International Conference on Future Networks and Distributed Systems,* edited by Mohammad Hammoudeh (Association for Computing Machinery, New York NY United States, 2023), pp. 377–383.
20. Malikov Z. M. et al., Comp. Res. Modeling. **T. 16, №. 2**, 395-408 (2024).
21. Malikov Z. M., Kh N. F., Herald Bauman MSTU, Ser. Nat. Sci., **2 (101)**, 22–35 (2022).
22. Malikov Z. M., Nazarov F. K. Comp. Res. Model. **13 (4)**, 793-805 (2021).
23. F. K. Nazarov, S. M. Khasanov and A. A. Yakubov, IJRTE **8 (4)**, 2140–2144 (2019).
24. Turbulence modeling Resource. NASA Langley Research Center. http://turbmodels.larc.nasa.gov
25. D. Anderson, J. Tannehill, and R. Pletcher, Computational Fluid Mechanics and Heat Transfer, Third Edition (2016).